Energy 90 (2015) 796–806

Contents lists available at ScienceDirect

Energy

journal homepage: www.elsevier.com/locate/energy

Piezoelectric energy harvesting from raindrop impacts

Mohammad Adnan Ilyas*, Jonathan Swingler

School of Engineering and Physical Sciences, Heriot-Watt University, EH14 4AS, United Kingdom

ARTICLE INFO

Article history:
Received 2 February 2015
Received in revised form
24 July 2015
Accepted 26 July 2015
Available online 29 August 2015

Keywords:
Energy harvesting
Piezoelectric
Raindrop

ABSTRACT

PEH (piezoelectric energy harvesting) techniques can be used to capture vibration, motion or acoustic noise, to be converted in to electrical output. In recent years there has been an increased interest in scavenging energy using alternative sources. This study focuses on the impact of raindrop on a PEH device and the possibility of harvesting energy from this source. Impact of water droplets on a PEH are analysed after having been released from various heights to replicate a rain shower. Detailed experimental results show features which have not been published in the literature before. The results show two distinct stages in the voltage and power output; first, a log growth, then an exponential decay during an impact event. A model is also developed to characterise the output power for one unit device which is then applied to an array of rain impact harvesters. The experimental results show a power output for one unit at around 2.5 μW that is typical of the data produced in other publications. However, there is significant room for improvement as the efficiency of the system is found to be no more than 0.12% of the total kinetic energy in a typical raindrop in freefall.

1. Introduction

EH (energy harvesting) is a process whereby energy is captured from external sources such as solar, wind or other means. The challenge is to provide efficient and "clean" power for micro to macro level applications. EH techniques at the micro-level can mainly be categorised into three forms: piezoelectric, thermoelectric and photovoltaic. The present study examines harvesting energy from raindrop impact using a PEH (piezoelectric energy harvesting) device.

PEH devices use vibrations, motion or acoustic noise as the source of external energy which can be converted to electrical energy. These are typically used for application with low power requirements such as powering sensor equipment from ambient vibrations [1], MEMS (microelectromechanical systems) [2], wireless sensor [3], and military applications [4]. Although significant progress has been made in this field in the development of microscale power supplies, power management and consumption, there remains a need to improve these further with the advent of the "Internet of Things".

A piezoelectric material is capable of producing an electric charge when the material undergoes mechanical stress. There are many materials such as quartz and tourmaline crystals that exhibit this piezoelectric effect. Such materials have in the past been actively used as electromechanical transducers [5]. The ferroelectric group of materials which exhibit the piezoelectric effect are also known as piezoelectric materials. Ferroelectric ceramics such as PZT (lead zirconate titanate) are widely used in EH due to their favourable properties and much discussion can be found in the literature on these, for example [6,7]. PZT devices have been considered to be a prospective replacement for batteries in some applications due to their high piezoelectric character and energy output. Organic materials such as PVDF (polyvinylidene fluoride) are mainly used in applications requiring a higher degree of mechanical flexibility and optical transparency. These polymers are relatively cheap and can be easily integrated into various applications; in garments or shoes [8]. These polymers also exhibit unique features such as demonstrating excellent mechanical behaviour, being corrosion resistant, having the ability to withstand stress without structural fatigue and illustrating an ease of processability on dielectric thin films. In particular, these polymers have the potential to be integrated into flexible devices [9].

The focus and novelty of this study is to show the behaviour of a harvesting system scavenging energy from raindrops. Three points in particular have been found from the work:-

- A detailed voltage output profile from the piezoelectric device shows that there is an initial impact stage and a decay stage with

* Corresponding author.
E-mail addresses: a.ilyas@hw.ac.uk (M.A. Ilyas), j.swingler@hw.ac.uk (J. Swingler).

http://dx.doi.org/10.1016/j.energy.2015.07.114
0360-5442/

an oscillatory character to the harvesting event of an impact. These features have not been demonstrated until now.
- The initial impact stage, of the interaction mechanism between the droplet and device, lasts for a significant period when compared to the duration of the entire harvesting event.
- The power output is at a very low level and is consistent with other researchers' work. However, the efficiency is found to be very small as well, providing an opportunity for future improvement of the transfer function of the device, for example, by modifying the harvester's surface.

1.1. Raindrop energy harvesting

EH from the impact of raindrops has been gaining significant research interest over recent years by a handful of groups, and the potential still has not been fully unlocked. It is this REH (raindrop energy harvesting) that is the focus of this study. Many geographical locations receive a moderate to heavy rainfall which can then be utilised to generate electricity as an alternative method to conventional and other mainstream renewable techniques. Energy output using such a system is very low in comparison to other forms of renewable power generation, but may be sufficient to power electronic devices in specialist low power applications where replacing batteries is not a feasible option. Additionally, the battery-less application is becoming more frequent because of the limitations due to size, weight, environmental impact and life of the battery. Applications like wireless micro-sensor networks [10] and MEMS (microelectromechanical systems) [11] are examples of such emerging technologies that have integrated energy harvesting methods.

The energy output in REH devices depends on the mass of the droplet, the velocity and the mechanism of impact at which it strikes the harvesting device. The radius of rain droplet can vary between 1 mm and 5 mm depending on geographical location and type of rain [12]. The maximum output reached experimentally using these techniques is 12 mW as detailed in Ref. [13].

1.2. Impact velocity

There are many factors that affect the output of a REH device. The key factors of the droplet are; volumetric size, mass, and velocity of impact. A raindrop in freefall towards the ground experiences two forces that are exerted vertically on it: a force acting upwards, known as the drag force, and the force acting downwards, the gravitational force resulting in the weight of the droplet.

The drag force on the droplet is represented in Equation (1), where ρ_a is the density of air, A is the projected frontal area of the droplet, v is the velocity of the droplet and C is the coefficient of drag.

$$F_{air} = \frac{1}{2}\rho_a A C v^2 \tag{1}$$

The weight of the droplet is represented in equation (2), where ρ_w is the density of the water droplet, r is the radius of the droplet and g is the acceleration of the droplet due to gravity.

$$F_{gravity} = \frac{4}{3}\pi r^3 \rho_w g \tag{2}$$

When these forces are in balance the droplet reaches its terminal velocity, v_T, the maximum velocity if no other forces act on the raindrop. This is shown in Equation (3), where d is the diameter of the droplet.

$$v_T = \sqrt{\frac{\pi d^3 \rho_w g}{6\rho_a A C}} \tag{3}$$

The assumption made in this study is that all rain droplets are spherical in shape. In reality, this can vary depending on the type of rain shower and the air resistance. Most experiments conducted under laboratory conditions, as reported in the literature, using a standard burette or pipette arrangement will typically have the diameter ranging between 0.5 mm and 2 mm, for which the droplet remains in a spherical shape. With an increase in the diameter of the droplet, it has been shown that the shape can change depending on wind speed and air resistance [14]; however that discussion is beyond the scope of this study.

1.3. Raindrop impact mechanism

The impact mechanism is another factor which will significantly influence the energy transfer function of the harvesting device and its power output. Generally, the impact mechanism of a droplet falling onto a solid surface can be divided into three main categories: 1) bouncing, 2) spreading and 3) splashing. The water droplet can either fully bounce leaving no water residue on the solid surface, which is depicted in Fig. 1a, or partially bounce leaving water residue, as depicted in Fig. 1b. The second category of the water droplet is spreading on impact, when the water adheres to the surface at impact, as depicted in Fig. 1c. The third category of the water droplet is splashing, when the droplet breaks into many parts and adheres to the surface. The droplet will then be distributed on the surface as depicted in Fig. 1d. The impact of a droplet on a harvesting device is expected to demonstrate all or a combination of these mechanisms. Studies have shown these types of droplet impact mechanisms on solid surfaces [15,16].

Various studies show the dominant impact mechanism of a water droplet is one that involves splashing [14]. An empirical relation as represented in Equation (4) is developed by Stow et al. [17] and by Mundo et al. [18] from experiments, where R_e is the Reynolds number (a dimensionless number defined as the ratio of inertial forces to viscous forces), W_e is the Weber number (a dimensionless number with relative importance of fluids inertia compared to surface tension) and K defined as a constant (which depends on the roughness of solid surface and thickness of layer).

$$K = W_e^{\frac{1}{2}} \times R_e^{\frac{1}{4}} \tag{4}$$

The Reynold's and Webber's numbers are found from the equation (5) below where ρ_w is the density of fluid, μ_a is the viscosity, σ is the surface tension of the fluid and v is the velocity:

$$Re = \frac{\rho_w v d}{\mu_a}; \quad We = \frac{\rho_w v d}{\sigma} \tag{5}$$

It was proposed that the behaviour of the water droplet can be determined by Equation (4), which will either deposit on the surface or splash. If K is found to be smaller than a particular K_c, a

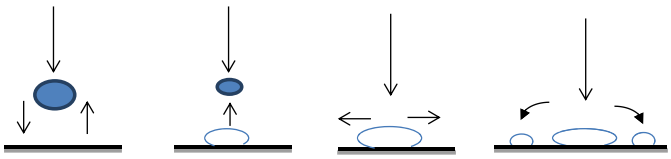

Fig. 1. Water droplet impact on solid surface.

threshold value, then only deposition will occur, and if K is greater than this K_c then a splash will develop [19].

A study of the impact of a water droplet should also consider whether the impacted surface is horizontal or inclined. Investigations conducted by Sikalo et al. [20,21] analyse the theoretical and experimental results of horizontal and inclined surfaces. The effect on horizontal surface was found to be mainly due to surface material properties, impact velocity, droplet viscosity, droplet surface tension and droplet size. The surface of impact plays an important role where the maximum spread is large on a glass surface in comparison to wax and PVC (polyvinyl chloride). The maximum spread and spreading velocity increases with increasing the impact velocity. Water, isopropanol and glycerine droplets are used in the experiments with nearly the same Webber and Reynolds numbers. The results of the experimental study formulated the empirical model of impacting droplet–surface interaction. The maximum spread increases with increasing Reynolds and Weber numbers. Another study [21] reviewed the impact onto an inclined surface which was dependent on droplet material properties such as viscosity, density and surface tension. The rebound effect could only be achieved on a dry smooth glass and on wetted surfaces. There was no rebound on wax and rough glass. It was concluded that the temperature of droplet and surface has no significance on the bouncing or spreading of droplets.

The objective of this study was to investigate the conversion of water droplet kinetic energy using a PEH device to convert the impact and vibrational energy of the device into electrical energy. As the droplet fell from standstill it accelerated along a path increasing in velocity. As discussed previously, the droplet can reach equilibrium at a certain stage as represented by Equation (3). The kinetic energy of the droplet is then related to the velocity and droplet size as shown in Equation (6).

$$E_{KE} = \frac{1}{2}\rho_w \left(\frac{4}{3}\pi\left(\frac{d}{2}\right)^3\right) v^2 \tag{6}$$

The droplet harvester is not expected to be able to extract all this energy, even if it is an optimised harvester, however, a Betz type limit is expected to apply as deposits on the harvester need energy to be removed.

1.4. Behaviour of rain

Rain and other forms of precipitation occur when warm moist air cools and condenses. This happens as a result of moisture condensing to liquid, as warm air can hold more water than cool air. Also, rain can be categorised into convection or stratiform. The cycle of convection mostly occurs in regions closer to the equator where the moisture in the ground is heated above the temperature of the surrounding areas, leading to an increase in evaporation. As the water vapour rises, this condenses into clouds which then subsequently can produce rain. The resulting convective shower mostly occurs for a short period of time over a limited area. Areas surrounding the equator are most likely to receive regular convective showers. For example, in the UK this phenomenon is referred to as 'sunshine and showers' as it rains in a smaller area followed by clear spells. This type of rain mostly occurs in the South and East of the UK [22].

Stratiform rain occurs when warm and cold air meet, but do not mix easily since they have different densities. Normally under these conditions the warm air rises over the cold air creating a 'front'. When air is forced up a mountainside, the water vapour in that air then condenses and falls as raindrops. Generally warm fronts are followed by light showers. The duration of stratiform rainfall is less but the intensity can be high [22].

Stratiform rain is further categorised into 3 types: LSR (light stratiform rain), MSR (moderate stratiform rain) and HT (heavy thunderstorms). Some typical values of raindrop size and velocity measured by Perera [14] are presented in Table 1.

1.5. Recent raindrop impact harvesters

One of the earliest studies conducted on REH (raindrop energy harvesting) [23] recommended the use of harvesting devices based on impact of raindrops. For remote areas and cities not connected to the grid system, the emphasis has been on renewable energy primarily in the form of solar systems. Solar systems are more effective during a sunny spell but prove ineffective during monsoon season. Bangladesh, which routinely has around 4 months of a monsoon season, could find the implementation of a REH system to be very beneficial. The study also contributes a detailed rain pattern in Bangladesh and a positive energy output of various energy harvesting techniques, depending on the impact velocity and drop size.

One of the most significant studies carried out on REH [12,13] in which the authors conducted extensive research on theoretical and experimental models. The piezoelectric material selected for the study was PVDF given its favourable lightness, flexibility and environmentally friendly properties. The theoretical study estimated the energy that could be harnessed during the impact of a raindrop. To reduce the weight and increase the efficiency, a single sheet of PVDF was used rather than the combination of two sheets. A mechanical-electrical transient model was developed to predict the behaviour of a piezoelectric cable device. The experimental phase of the project focuses on impact simulation of a piezoelectric sheet. By using the mechanical-electrical model, the authors were able to achieve conclusive results on the energy harvested. By using various drop heights and drop sizes, 1 nJ of electrical energy and 1 μW of instantaneous power was harnessed as a minimum. By artificially creating a downpour, the energy harnessed was 25 μJ with a power output of 12 mW.

Another study [24] looked at harvesting energy from rainfall using commercial transducers. Experiments were conducted on the two materials PZT and PVDF as a means of drawing a beneficial comparison. The transducers were exposed under rain to determine the voltage levels generated by the impact of rain droplets. The study recommended the use of PVDF transducers for REH devices because they generate high power, have a lower cost and are not toxic when compared to PZT transducers.

Another study [25] focused on a device with a combination of cantilevers and diaphragm structures forming the REH. A comparison of empirical and simulation data was presented. The prototype developed for the energy harvester consisted of several layers namely: silicon, polyamide, Al (aluminium), and the PVDF active layer. The focus in this research was on a meshed model of the harvester. Results show a displacement pattern for the centre of the diaphragm with various thicknesses of Al and PVDF. To achieve

Table 1
Rain types [14].

Rain type	Drop size (mm)	Terminal velocity (m/s)
Light stratiform rain		
Small	0.5	2.06
Large	2.0	6.49
Moderate stratiform rain		
Small	1.0	4.03
Large	2.6	7.57
Heavy thundershower		
Small	1.2	4.64
Large	4.0	8.83
Largest	5.0	9.09

optimum results, thinner Al and PVDF are used, as thickness is inversely proportional to maximum displacement. On the cantilever surface, as the thickness of PVDF is increased the maximum displacement begins to decrease whereas the Al is directly proportional to the maximum displacement. It is concluded that PVDF thickness of 150 μm and Al thickness of 35 μm results in a maximum displacement of 2800 μm. However, at these thicknesses the maximum displacement on the centre of the diaphragm is relatively small. These thicknesses are able to withstand the impact pressure of a large droplet of 13.718 MPa. The maximum displacement limit is found to be 2800 μm.

A review [26] looked at the limited studies conducted on PZT and PVDF harvesters using droplet impulses. The study also included a comparison of the results obtained from a bridge and cantilever structure using a PVDF film. The experimental results illustrated that the cantilever structure only produces a few millivolts as the structure is soft and easily deformed, whereas the bridge structure produced a higher voltage. The design of the bridge structure was supported at both ends, thus rendering it more rigid. The maximum voltage produced in the bridge structure was around 3.502 V in whereas the cantilever structure registered a corresponding maximum figure of 1.003 V. It was also observed that droplets pass through the cantilever structure and splash on the ground whereas on the bridge structure the droplets impact and splash on the beam, thereby absorbing more energy.

2. Experimental arrangement

2.1. Material and device specification

A commercially available piezoelectric sensor by Pro-Wave (FS-2513P) was used in this study. This device was chosen as it has PVDF as the active piezo film which has been identified as an ideal piezoelectric material with favourable properties for the impact of water droplets. The piezo film was protected by a transparent non-conductive coating. Ag (Silver) electrodes are plated on the top and bottom of the piezo film. The device has low mechanical and acoustic impedance, and has a high resistance to moisture. Connecting wires are soldered onto the end terminals to contact the load and measure the voltage output. The specification of the device is presented in Table 2.

2.2. Experimental tests

The device was clamped at one end as shown in Fig. 2 and the clamping position for all measurements remains constant throughout the study. Raindrops were artificially replicated in the laboratory by the use of a burette and set to produce drops at a constant size and rate. The radius of the droplet at the instant before it is released from the burette was measured to be 2 ± 0.2 mm. It is assumed the water droplet is spherical just before impact with the harvester device. The water droplets were aimed at the centre of impact zone on the device as shown in Fig. 2. The distance covered by the water droplet from the position it was released from the burette to the surface will be referred to as the impact height, h, for the purpose of this study.

Table 2
Piezo device specification.

Dimensions	25 × 13 × 3 mm
Capacitance	1.5 ± 30% nF @ 1 KHz
Resonant frequency (Fr)	80 ± 10 Hz
Voltage sensitivity at Fr	70 mV/ms^{-2}
Operation temperature	−20 to +60 °C

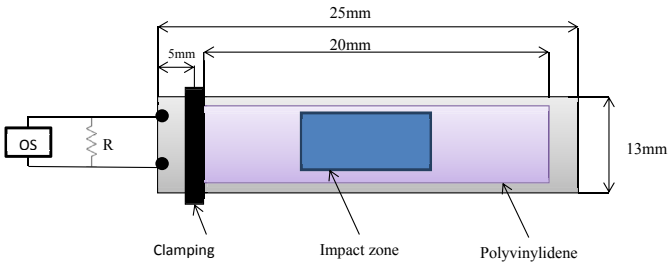

Fig. 2. Piezo device positioned under a burette.

The output from the piezo device was measured using a Digital Oscilloscope (Tektronix – TDS3032B) with Differential Probes (Testec-TTSI9001). Resistive loads of 1 MΩ (±5%), 1.8 MΩ (±5%), 2.2 MΩ (±5%), 2.7 MΩ (±5%), 3.3 MΩ (±5%) and 4.7 MΩ (±5%) were connected as appropriate. The output voltage was measured under impact of water droplets for each of the loads. Each test was repeated several times for reproducibility of data.

3. Results and analysis

The results and analyses are presented in three sub-sections. The first sub-section gives an example of the type of raw data acquired by the investigation. The subsequent two sub-sections are analyses of the two main features observed in the data of any one single event.

3.1. Raw data and the event

Fig. 3 shows the profile of the voltage output from the device once a droplet impacts that device. Several features in the resultant sinusoidal oscillations can be observed and will be discussed later in detail with Fig. 4 (which shows the volt and time units). Fig. 3 shows the device sensor deflection position (which is derived from the voltage output) as well as showing the voltage output. Before the water droplet impacts the device, the piezo sensor is at a horizontal position illustrated in Fig. 3 close to the zero position. As the water droplet falls onto the sensor, it interacts with the sensor and starts to push the sensor downwards from position 1 the "Droplet impact start sequence" to position 2 the "Maximum negative velocity of device sensor". The sensor accelerates during this time and reaches a maximum negative velocity at position 2 resulting in a maximum negative voltage. The sensor then decelerates and reaches its full deflection at position 3 the "Full deflection of device sensor" resulting in a zero voltage. The device sensor then starts to rebound and accelerate back in the opposite direction and reaches its maximum positive velocity at position 4

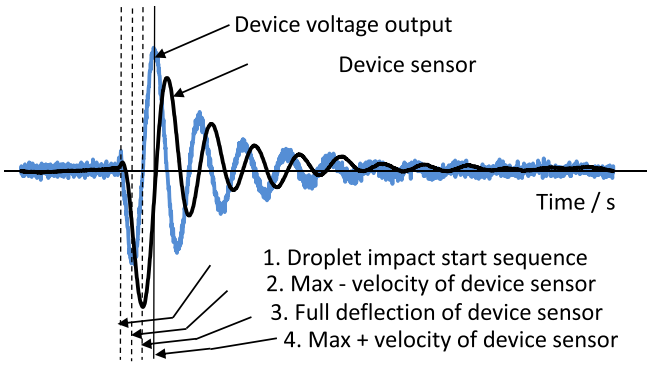

Fig. 3. Voltage output and sensor position profiles of the device.

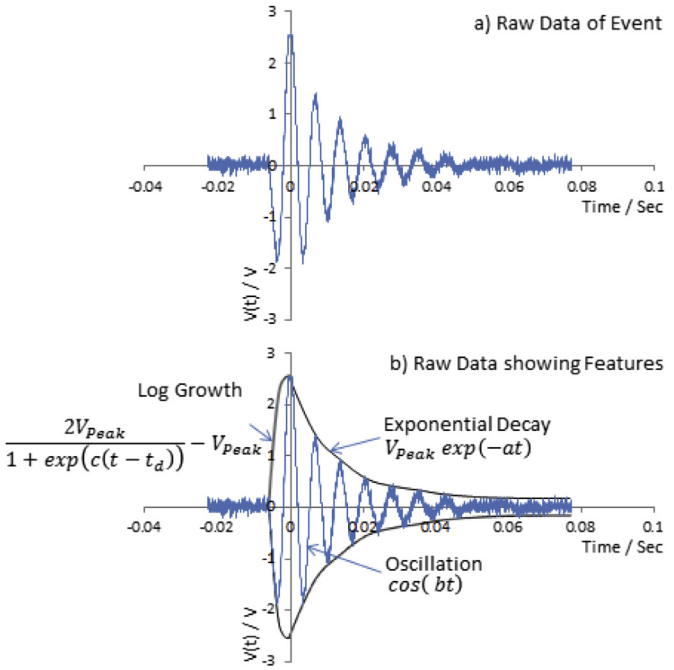

Fig. 4. Voltage output of harvester for one event (Raw data).

the "Maximum positive velocity of device sensor". This results in a maximum positive voltage output which is the maximum voltage magnitude of the whole event. After this point in the whole event, the voltage output oscillations and deflection oscillations of the sensor decay away.

As was expected, the first deflection of the sensor in the negative position when pushed down by the droplet impact was the largest maxima of all subsequent maxima of the oscillations. It should be noted that the droplet does not deliver all its energy at the first instant of the impact but takes a finite time as the droplet interacts with the device sensor. The impact mechanism is complete and available energy fully delivered when the full deflection of the device sensor is reached at position 3 in Fig. 3.

Fig. 4a depicts the voltage output profile of a single energy harvesting unit of a water droplet impact event. An oscillating profile is shown which consists of two stages as the event evolves with time. These stages are shown in Fig. 4b as the "log growth" stage as the voltage grows to a maximum followed by the "exponential decay" stage as the voltage decreases to zero.

The oscillating profile is of a cosine form which is seen in the two stages. The log growth stage in the voltage consists of a growth term and the cosine term as shown in Equation (7), where V_{Peak} is the highest voltage attained, t_d, c and e are constants:

$$V(t) = \left(\frac{2V_{Peak}}{1+exp(c(t-t_d))} - V_{Peak}\right)cos(et) \quad (7)$$

The exponential decay stage of the voltage consists of a decay term and the cosine term as shown in Equation (8), where a is related to the half-life of decay, $t_{1/2}$ and b are related to oscillation frequency f as shown in Equation (9):

$$V(t) = V_{Peak}exp(-at)cos(bt) \quad (8)$$

$$V(t) = V_{Peak}exp\left(-\frac{In(2)}{t_{1/2}}t\right)cos(2\pi ft) \quad (9)$$

3.2. Log growth stage

During the log growth stage of the harvesting event, the voltage grows to a peak V_{peak}. A plot of this peak voltage against load, R, for different impact heights is shown in Fig. 5. This shows that by increasing the impact height the peak voltage output also increases. It can also be seen that as the load is increased the peak voltage also increases. A best fit linear regression is found for each profile with a correlation coefficient (the R-Squared parameter) between 0.43 and 0.90.

Fig. 6 depicts the power and energy output of the log growth stage of one event for different impact heights at different loads. Mean power against load is also plotted as shown in Fig. 6a, which is consistent with the expectation of higher power with an increase in the impact height. At different loads the mean power for 17 cm and 27 cm droplet heights is reasonably consistent between 0.2 and 0.6 μw. There is an outlier in the data captured for 37 cm which shows a decrease in the mean power when the load is 1.8 MΩ; however the rest of the data on 37 cm is reasonably consistent. Impact height of 47 cm shows an increase in mean power with increasing load up to 2.2 MΩ but the mean power decreases with a further increase in load over 2.8 MΩ.

The duration of the log growth stage for the events is shown in Fig. 6b. No trend is observed in this data in relation to droplet height or loading. The duration for this stage of the event, t_{d1}, is approximately 6 ms.

Fig. 6c shows the energy harvested during the growth stage of the event (product of data in Fig. 6a and b).

3.3. Exponential decay stage

During the exponential decay stage of the harvesting event, the voltage oscillations decay away. The decay constant and time constant, the coefficients 'a' and 'b' for Equation (8), for this are found and plotted in Fig. 7. As can be seen, the influence the impact height and the load, R, have on these coefficients shows no clear trend within the resolution of the experiments. Trend lines have been fitted to all collected data points.

Fig. 7a shows that the decay constant, a, across all loads, is approximately 60 s^{-1} which is a half-life, $t_{1/2}$, of 0.0115 s. Fig. 7b shows that the time constant, b, across all loads is approximately 900 s^{-1} which is an oscillation frequency 143 Hz.

Fig. 8 shows the power and energy output of the exponential decay stage of one event for different impact heights at different loads. The plot of mean power against load is once again reasonably

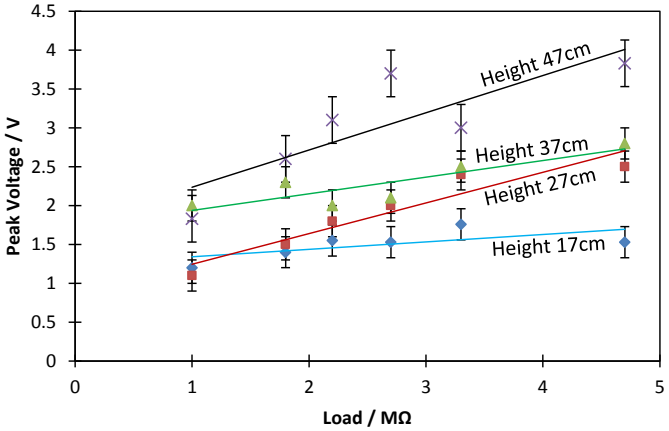

Fig. 5. Voltage peak (V_{peak}) from harvester.

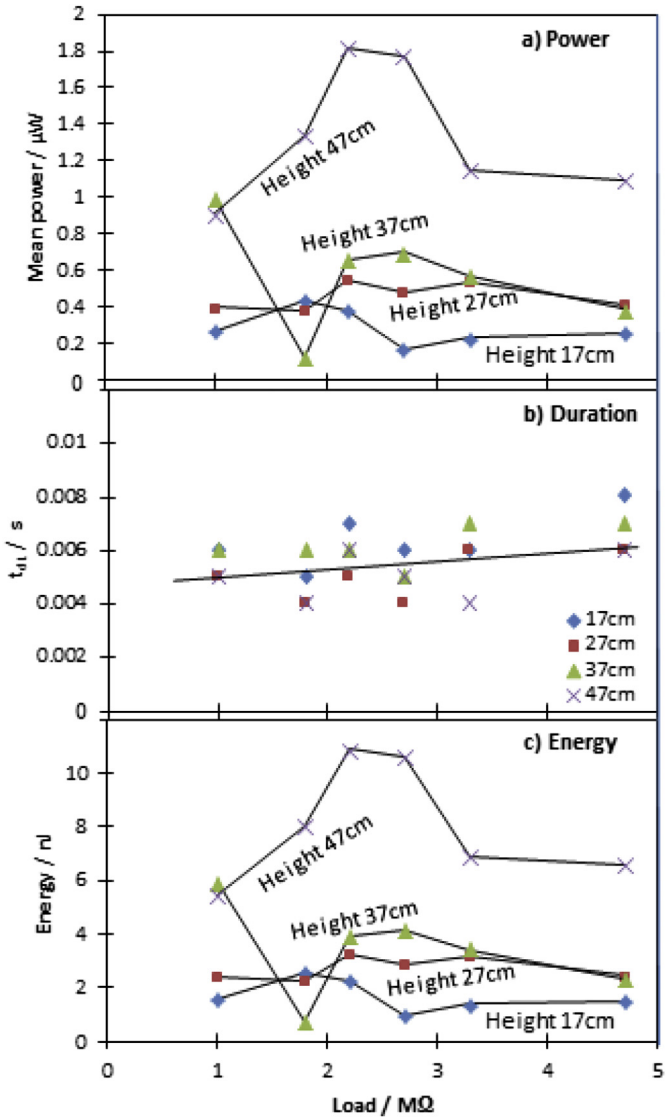

Fig. 6. Power & energy output of the log growth stage of one event.

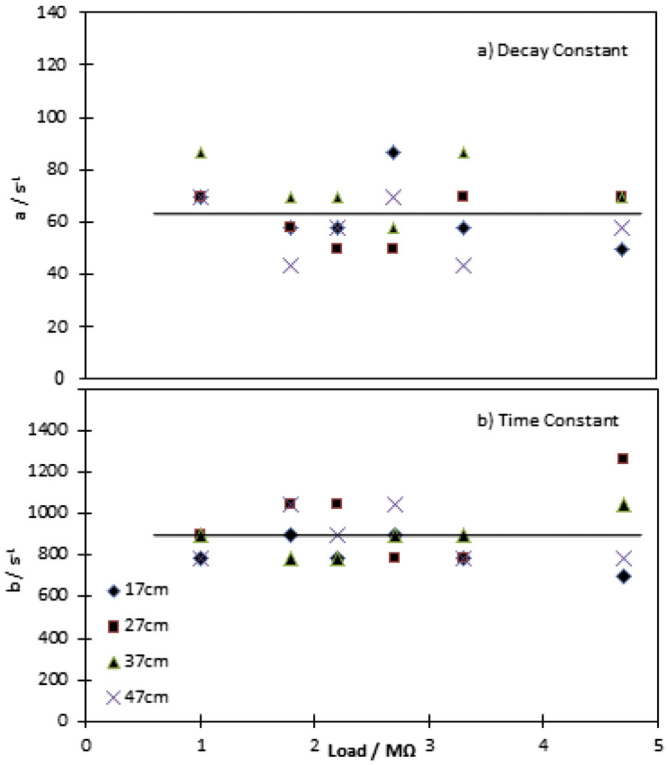

Fig. 7. Exponential coefficient 'a' and cosine coefficient 'b'.

consistent with the trend of higher power with an increase in the impact height as shown in Fig. 8a. Impact height of 47 cm shows an increase in power with an increase in load from 1 MΩ to 2.2 MΩ. However the power output starts to decrease if the load is increased over 2.2 MΩ. There is an outlier in 37 cm impact height, which shows the maximum power at 1 MΩ and then decreases as the load increases. Power values for 17 cm and 27 cm are reasonably consistent.

Fig. 8b shows the duration of the exponential decay for different impact heights and loads. Trend line has been fitted to all collected data points. The duration of this stage of the event, t_{d2}, is approximately 30 ms.

Fig. 8c shows the energy harvested during the decay stage of the event (product of data in Figs. 8a and 6b).

The mean power during stage 2, the decay stage, is around 30% smaller than the growth stage. The average time duration of 0.006 s for the growth stage is 20% that of the decay stage. The energy of the growth stage is around 69% that of the decay stage. All this shows that in the growth stage of the event, the impact process of the droplet, has a significant contribution to the overall output of the device.

4. Discussion and energy harvesting modelling

The discussion starts by dealing with the data collected from the single harvesting unit as a complete system. A calculation of the droplet velocity is made to relate the voltage output to the droplet velocity under different electrical load conditions. The second sub-section examines how the experimental data evolves with time giving rise to the mean power and energy from one unit during one event. The third sub-section proposes a multi-harvester array by using the data from the single unit and examines the expected output from multi-events of raindrops with time. The final sub-section then critically evaluates how realistic the experimental results are compared to real rainfall, while giving consideration to its possible applications and any issues arising from the study.

4.1. The harvesting system

A full understanding of an EH system requires a description of a) the input to the harvester, b) the harvester's converter processes and c) the output to a load or consumer.

The energy input to the harvester from a droplet impact is related to the kinetic energy of the droplet and the impact mechanism giving rise to an energy transfer function/coefficient. The kinetic energy, as described by Equation (5), is a function of the density of the droplet, its radius and the square of its impact velocity.

A numerical method, based on Equations (1) and (2), was employed to relate the height, h, of the droplet to its expected velocity, v, on impact with the device. The density of air and water are taken to be 1.2041 kg/m^3 & 999.97 kg/m^3 respectively, the droplet is considered to be a sphere of radius 2 mm, and the drag coefficient is considered for a sphere of 0.47. Velocity profiles are illustrated in Fig. 9. It can be seen in Fig. 9a that a terminal velocity of 9.62 ms^{-1} is attained if the droplet is allowed to fall for more

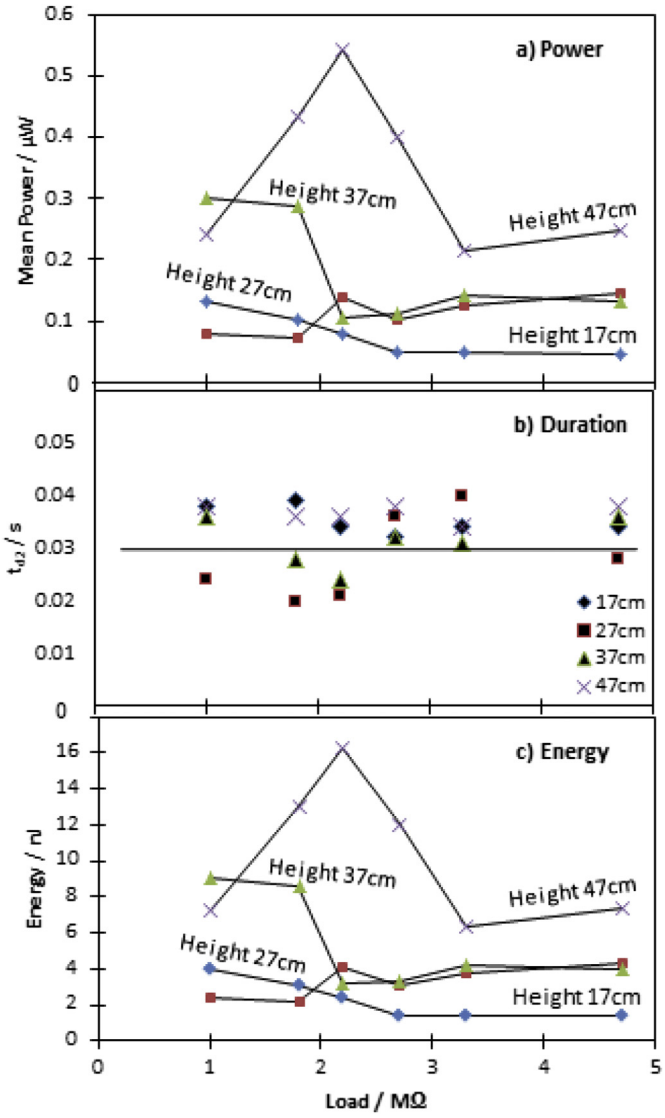

Fig. 8. Power & energy output of the exponential decay stage of one event.

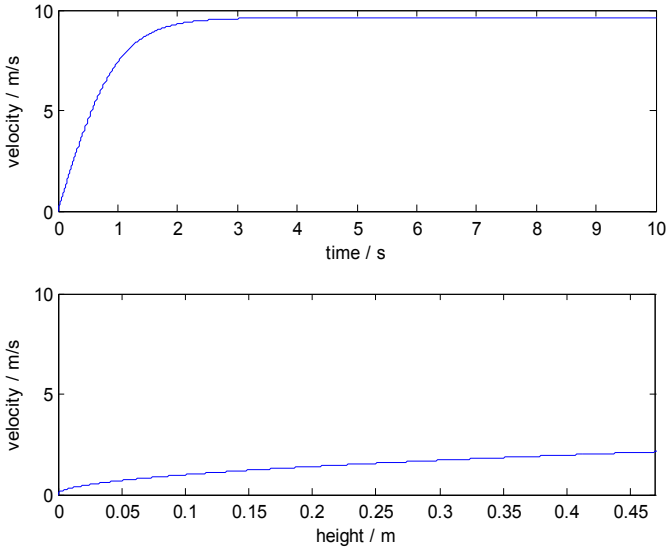

Fig. 9. Relating droplet fall height to velocity.

than 3 s. In the experiments conducted, at a maximum height of 47 cm, the velocity expected to be achieved is 2.13 ms^{-1}, as shown in Fig. 9b.

Fig. 10a shows the relationship between the peak voltage produced by the device and the expected velocities of the droplets on impact from the experiments conducted under different electrical loads. Clear trends are seen and gradients of best fit lines are found with coefficient of correlation ranging from 0.63 to 0.94. These gradients of peak voltages per impact velocity are plotted against the electrical loads in Fig. 10b, to give a volt per impact characteristic.

From the experimental data as given in Fig. 10, an empirical relationship between the peak voltage and raindrop impact velocity is given in Equation (10). A power law fit is used as this had a best fit with a coefficient of correlation of 0.97.

$$V_{peak} = M_R \frac{R^n}{R_0} \nu \tag{10}$$

where ν, the velocity, which is dependent on the impact height, R is the external electrical load, R_0 is a constant to conserve units of value 1 Ω^n and M_R is the volt-impact coefficient. From the analysis of the data in Fig. 10 the following parameters are found: $M_R = 0.0054\ Vsm^{-1}$ & $n = 0.3714$. These values are used to calculate the peak voltage to model the voltage profile over an event. This is discussed hereafter.

4.2. One unit harvester and one event

The experimental data acquired is from a single unit harvester and the analysis focuses on the profile of an event (repeated many times) which typically lasts for a total 0.036 s. The mean power of an event caused by different impact velocities is calculated from the

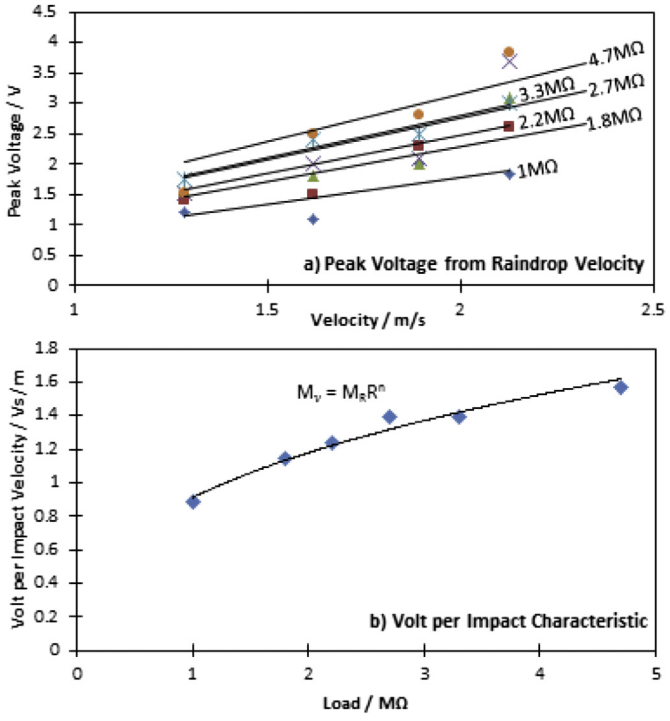

Fig. 10. Volt per impact characteristic.

data as shown in Figs. 6 and 8, the power of the log growth stage and the decay stage. This total mean power is plotted in Fig. 11a which is found to be generally below 2.5 μw. Energy is plotted in Fig. 11b which is found to be generally below 90 nJ. The efficiency of the experimental data, shown in Fig. 11c, is also very low. These are very low values making it questionable whether such a harvesting technique can be of any practical use.

The efficiency is also found to be extremely low at generally less than 0.12%. However, there is opportunity for significant improvement which may lead to this technique being a viable option for specialist applications. The efficiency of piezoelectric harvesters has been studied under constant oscillations by Shy et al. [27] which give a value of up to 18% efficiency and potentially up to 46% efficiency. This indicates that higher efficiencies can be achieved. Areas which can be addressed to improve this in the current techniques are: a) the energy transfer function of the impact mechanism on the harvester, b) the harvester's conversion processes of the piezoelectric material, and c) the output load matching.

The impact mechanism is one area which is critical for the voltage output and efficiency of the harvester. The importance of this is highlighted in section 1.3 and controlling this mechanism will give opportunities for development. One of the assumptions made in the model is that all raindrops behave the same on impact. A detailed investigation is beyond the scope of the present study; however this is currently under further investigation.

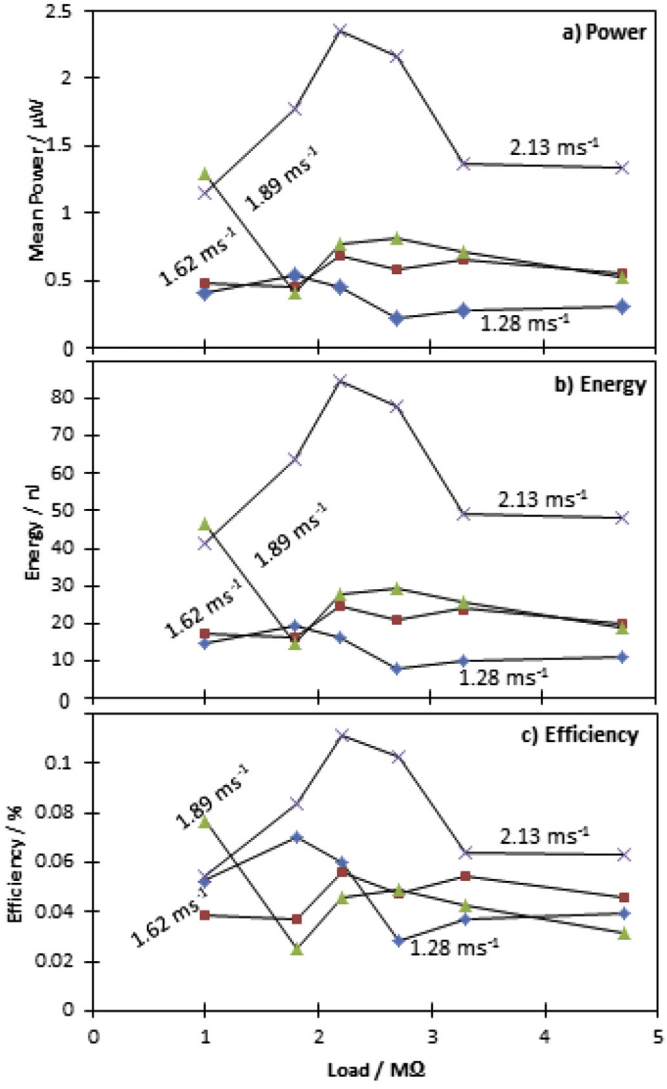

Fig. 11. Output of the device.

Load matching is always important for electrical devices. The peak in the efficiency data of the 2.13 ms^{-1} profile may be due to the load being appropriately impedance matched. Further work is required in this area.

Having multiple harvester units, given appropriate design constraints, will enable more power to be delivered. Once a model of a single harvester unit is available, this can be used to scale up to an array of units. In this study, the mean power from one event has also been empirically modelled to obverse trends in the data which is used for building a harvester array model.

The calculation of the instantaneous power output from the harvester from one event is modelled as in Equation (11) combining Equations (7)–(9). Values for this instantaneous power can be found by using data from the results acquired.

$$P_{inst} = \left|\frac{1}{R_{load}}\left(\frac{2V_{Peak}}{1+exp(c(t-t_{d1}))} - V_{Peak}\right)^2 cos^2(2\pi ft)\right|_{t<0} + \left|\frac{V_{peak}^2}{R_{load}} exp^2\left(-\frac{In(2)}{t_{1/2}}t\right) cos^2(2\pi ft)\right|_{t\geq 0} \tag{11}$$

Equation (11) can be combined with equation (10) and integrated over the event duration.

$$P_{mean} = M_R^2 R^{-0.2572} v^2 \tau \tag{12a}$$

$$\tau = \int_{t_{d1}}^{0} \left(\frac{2}{1+exp(c(t-t_{d1}))} - 1\right)^2 cos^2(et)\,\frac{dt}{-t_{d1}} + \int_{0}^{t_{d2}} exp^2(-at)cos^2(bt)\frac{dt}{t_{d2}} \tag{12b}$$

where τ is the integration, resulting in $\tau = 0.5169$, and the other parameters are taken from the experimental results of a = 60; b = 900; c = −1200; e = $2\pi\ 3/(4t_{d1})$; $t_{d1} = 0.006$ s; $t_{d2} = 0.03$ s.

By using Equation 12a, a graph of mean power against the load is presented in Fig. 12.

This modelling approach loses the fine detail of the expected behaviour within the range of loads studied but does show a general trend of decreasing power with load. Also, it can be seen that the influence of impact velocities is appropriately modelled by comparing Fig. 11a with Fig. 12. This approach is used in the next section of modelling the output from an array of these harvester units.

4.3. A harvester array

Equation (12a) is used to model the behaviour of a unit harvester, based on the empirical data acquired in this study, and implemented in an algorithm to model a harvester array. A numerical approach is used for multiple units in an array of defined size for a rainstorm of particular duration and quantity. Fig. 13 represents the mean power output for a load of 1 MΩ, with rainfall of 32 mm (quantity of 32 L per cubic metre) and a duration of 300 s Fig. 13a shows the power output for a 1 m^2 harvester array to a resolution of 0.036 s (the duration of one event). It should be noted that the whole area of the array is not considered as actively harvesting but only a proportion of it. In this study the relevant

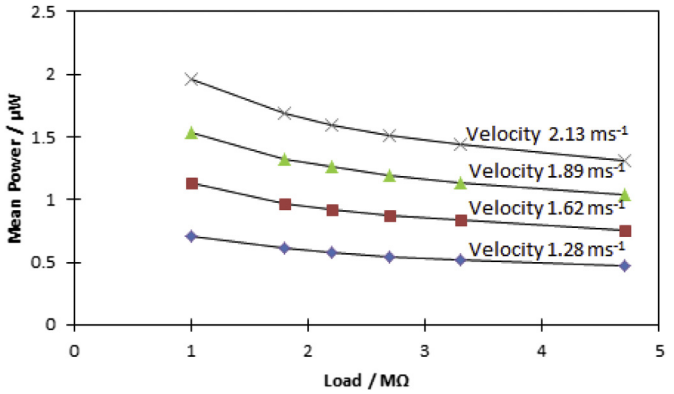

Fig. 12. Mean power found from model.

proportion is taken to be 80%. From Fig. 13a, it can be seen that the power output is "noisy" due to the random nature of rainfall. However the probability of the power output dropping below 100 µw is remote. Fig. 13b shows the distribution of expected power output (a frequency plot of the number of units of power within 0.036 s resolution) with a mean of 150 µw. Fig. 13c shows the power output for a 10 m^2 harvester array with its respective distribution plot. It can be seen that the noise or deviation from the mean is lower with large arrays.

As the size of the array is increased, power output is increased as a result, with the highest power of 160 mW and 3.5 W for different velocities attained at a 100 m^2 array as shown in Fig. 14a and c. With an increase in the size of the array, the noise to signal ratio is reduced significantly with a change of size from 1 m^2 to 1000 m^2 as shown in Fig. 14b and d.

4.4. Experimental conditions and applications

The focus of this current study has been to show the behaviour of a harvesting system scavenging energy from raindrops. To this end the design of the experimental conditions has been carried out with the aim of replicating a typical raindrop. The size of the rain droplet varies between 0.5 mm and 5 mm depending on the type of rain as discussed in Section 1.4. The droplet size used in the experiments is chosen within this range at a radius of 2 mm. The droplet velocity is calculated to be as much as 2.13 ms^{-1} depending on the height from which the droplet is released. This allows for a conservative estimate of a raindrop velocity and thus less than under optimistic expected power output. The terminal velocity of 9.62 ms^{-1} is calculated in this study in comparison to 6.49 ms^{-1} for stratiform rain of similar droplet size as shown in Table 1.

One of the assumptions made in this study is that the raindrop fell from a low altitude and therefore the changes in temperature, air pressure, air density and gravity are ignored. Another assumption is that the raindrop maintains its spherical shape just prior to impact. The raindrop is also assumed not to be affected by any extraneous force such as wind. Since all experiments are conducted based on a single impact which lasts around 0.036 s, the model is limited to single impact and does not take into account multiple impacts occurring simultaneously. All raindrops behave similarly upon impact based on the model presented here. It is an empirical model based on the data acquired and is dependent on the impact behaviour. However, it was found from running the multiple array simulation with appropriate levels of rainfall that, multiple impacts within the 0.036 s time window are a rare occurrence.

Given these assumptions, the main forces acting on the drop are the air resistance and gravity as mentioned in Section 1.2. The main factor which may influence the velocity under these conditions is the shape of the raindrop but for the purpose of this study we have assumed that the raindrop maintains a spherical shape during freefall. In fluid mechanics, Re and We are dependent on the velocity at which the raindrop is travelling. When the radius of the raindrop increases, the drag coefficient decreases respectively. The drag coefficient is also dependent on the Reynolds number, as investigated by Edwards et al. [28].

Tap water is used in this study which has many nutrients and minerals [29] & [30]. However, rainwater generally contains fewer minerals in comparison to tap water [33]. The surface tension of tap water at room temperature (20 °C) is 0.072 N/m [31] and dynamic viscosity at room temperature (20 °C) is measured as 0.982 cP [32]. There is no easily accessible published data available as regards its surface tension and viscosity.

Given these assumptions and approach, it is thought that the experimental study presented would give a good, if conservative, estimate of possible power output from rain droplet energy harvesting using the unmodified commercially available PVDF device. The study highlights some interesting features in the voltage profile and energy output. Two distinct stages are identified: a growth stage during the impact process followed by a decay stage as energy stored in the harvester devices is dissipated. It can be seen that the

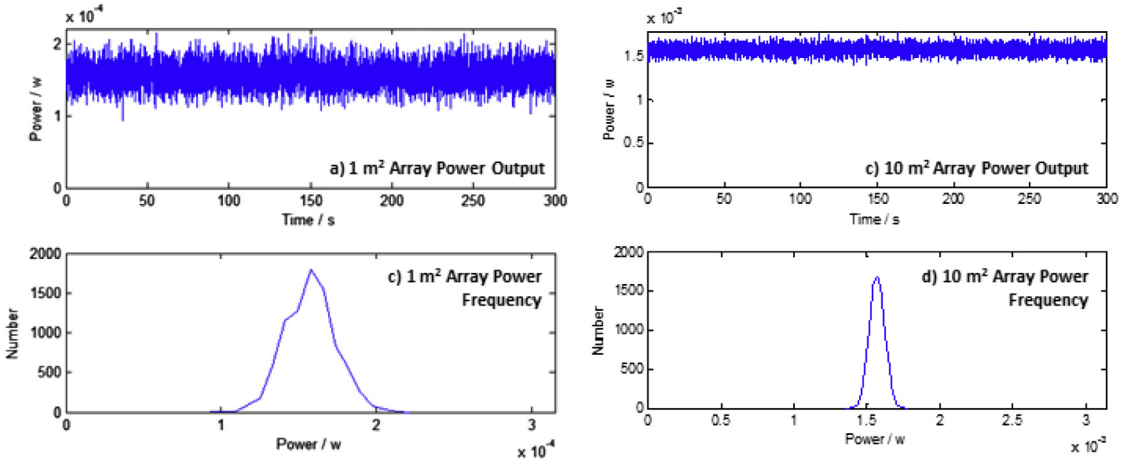

Fig. 13. Power output for harvester array.

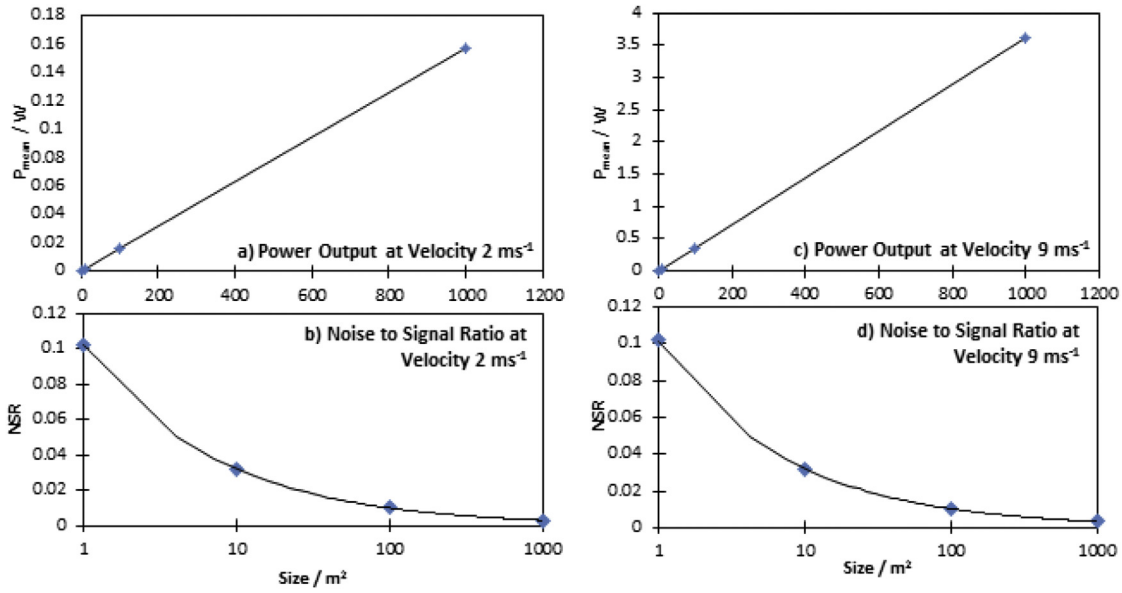

Fig. 14. Power output from array for different droplet impact velocity.

impact process lasts for a significant period of time and delivers a significant level of energy.

However, with the opportunity to improve the efficiently of the system, raindrop energy harvesters have many possible applications including self-powered sensors, wireless communication and hand-held devices as discussed in Section 1.1. Some other applications for this include powering medical devices which are isolated from power supplies and powering up telecommunications in remote areas. Many devices such as MP3 players, hearing aids and pacemakers use batteries as a source of power where the power consumption varies between 50 μW and 50 mW. The results of this study show we were only able to harvest power in the μW region and energy in nJ region. This study outlines REH technique using a single droplet impact and can be further improved to enhance the harvested power. An experimental study conducted by Guigon et al. [13] also reveals that approximately 1 nJ of electrical energy is recovered in a worst case scenario. As a result, simulations show that up to 25 μJ of energy is recoverable from a downpour.

5. Conclusion

This paper investigates an alternative approach to harvesting energy with piezoelectric materials by utilising raindrop impacts. Detailed experimental results with distinct features are presented highlighting the log growth and exponential decay of the harvesting process of a droplet impact. It has been shown that the droplet impact stage has a significant contribution to the overall power output of the device. The energy output of the device is found to be less than 90 nJ with the mean power below 2.5 μW for a single unit harvester during one impact event under different conditions. The efficiency is found to be low, generally registering less than 0.12%. However, it is thought that the efficiency of the device can be significantly improved by modifying the droplet impact mechanism with the harvester surface by exploring new surface materials to maximise inelastic collision. Future research will focus on other forms of surfaces (such as impact of hydrophobic surfaces) and its influence on the output and efficiency of the device.

A model has been developed which takes the empirical data for the single unit harvester during a single event and uses this for an array of harvesters with particular areas. Calculations for arrays of 1 m^2 and more are presented. The smaller arrays show larger noise to mean power ratios which demonstrates the random nature of rainfall.

This study has demonstrated the detailed behaviour of a harvesting system scavenging energy from raindrop impacts. Three main findings in particular have been highlighted in this work. 1) The detailed voltage output profile from the piezoelectric device shows that there is an impact stage during the droplet impact process, followed by a decay stage as stored energy in the harvester is dissipated, with an oscillatory character to the harvesting event of an impact. These features have not previously been identified. 2) The second main finding is that the impact stage lasts for a significant time period when compared to the duration of the entire harvesting event and has a significant amount of energy associated with it. 3) The final main finding is that the power output is very small and is consistent with the findings of other researchers. Nonetheless, the efficiency is found to be very small also, providing an opportunity for future improvement of the transfer function of the device, for example, by modifying the harvester's surface.

Acknowledgement

This work is partly funded by School of Engineering and Physical Sciences, Heriot-Watt University.

References

[1] Reily EK, Burghardt F, Fain R, Wright P. Powering a wireless sensor node with a vibration-driven piezoelectric energy harvester. Smart Mater Struct 2011;20.
[2] Trolier-Mckinstry S, Muralt P. Thin film piezoelectrics for MEMS. J Electroceramics 2004;12:7–17.
[3] Ottaman GK, Bhatt AC, Hofmann H, Lesieutre GA. "Adaptive piezoelectric energy harvesting circuit for wireless remote power supply. IEEE Transaction Power Electron 2002;17:669–76.
[4] Zakar E. MEMS piezo pressure sensor for military applications. U.S. Army Research Laboratory, Adelphi; 2004.
[5] Tilmans HAC. Equivalent circuit representation of electromechanical transducers: I.Lumped-parameter systems. Micromechanics Microengineering 1996;6:157–76.
[6] Lipscomb IP, Weaver PM, Swingler J, McBride JW. The effect of relative humidity, temperature and electrical field on leakage currents in piezo-ceramic actuators under dc bias. Sensors Actuators A Phys 2009;151(2):179–86.

[7] Lipscomb IP, Weaver PM, Swingler J, McBride JW. Micro-computer tomography-An aid in the investigation of structural changes in lead zirconate titanate ceramics after temperature-humidity bias testing. J Electroceramics 2009;23(1):72–5.
[8] Rocha J, Gonclaves L, Rocha P, Lanceros-Mendez S. Energy harvesting from piezoelectric materials fully integrated in footwear. IEEE Trans Industrial Electron 2010;57(3):813–9.
[9] Ramer N, Marrone T, Stiso A. Structure and vibrational frequency determination for α-poly(vinylidene fluoride) using density-functional theory. Polymer 2006;47:7160–5.
[10] Calhoun B, Daly D, Verma N. Design considerations for ultra-low energy wireless microsensor nodes. IEEE Trans Comput 2005;54(6):727–40.
[11] Hajati A, Kim SG. Ultra-wide bandwidth piezoelectric energy harvesting. Appl Phys Lett 2011;99.
[12] Guigon R, Chailout J, Jager T, Despesse G. Harvesting raindrop energy: theory. Smart Mater Struct 2008;17.
[13] Guigon R, Chailout J, Jager T, Despesse G. Harvesting raindrop energy: experimental study. Smart Mater Struct 2008;17.
[14] Perera K, Sampath B, Dassanayake V, Hapuwatte B. Harvesting of kinetic energy of the raindrops. Int J Math Comput Phys Quantum Eng 2014;8(2):325–30.
[15] Martin R. Phenomena of liquid drop impact on solid and liquid surfaces. Fluid Dyn Res 1993;12(2):61–93.
[16] Martin Rein. Introduction to drop-surface interactions. Drop-surface interactions. CISM International Centre of Mechanical Sciences, vol. 456. Springer Vienna; 2002. p. 1–24.
[17] Stow C, Hadfield M. An experimental investigation of fluid flow resulting from the impact of a water drop with an unyielding dry surface. In: Royal Society A: mathematical physical and engineering sciences; 1981.
[18] Mundo C, Sommerfield M, Tropea C. Droplet-wall collisions: experimental studies of the deformation and break-up processes. Int J Multiph Flow 1995;21(2):151–73.
[19] Josserand C, Zaleski S. Droplet splashing on a thin liquid film. Phys Fluids 2003;15(6):1650–7.
[20] Sikalo S, Marengo M, Tropea C, Ganic E. Analysis of impact of droplets on horizontal surfaces. Exp Therm Fluid Sci 2002;25:503–10.
[21] Sikalo S, Tropea C, Ganic E. Impact of droplets onto inclined surfaces. J Colloid Interface Sci 2005;286:661–9.
[22] Robert H. Stratiform precipitation in regions of convection: a meteorological paradox? Bull Am Meteorological Soc 1997;78(10):2179–96.
[23] Biswas P, Uddin M, Islam M, Sarkar M, Desa V, Khan M, et al. Harnessing raindrop energy in Bangladesh. In: International Conference on Mechanical Engineering, Dhaka; 2009.
[24] Viola F, Romano P, Miceli R, Acciari G. Harvesting rainfall energy by means of piezoelectric transducer. In: International conference on Clean Electrical Power, Alghero; 2013.
[25] Chin-Hong W, Dahari Z, Abd Manaf A, Sidek O, Miskam M, Mohamed J. Simulation of piezoelectric raindrop energy harvester. In: TENCON, Sydney; 2013.
[26] Wong C-H, Dahari Z, Manaf AA, Miskam MA. Harvesting raindrop energy with piezoelectrics: a review. J Electron Mater 2015;44(1):13–21.
[27] Shu YC, Lien IC. Efficiency of energy conversion for a piezoelectric power harvesting system. J Micromechanics Microengineering 2006;16:2429–38.
[28] Edwards BF, Wilder JW, Scime EE. Dynamics of falling raindrops. Eur J Phys 2001;22:113–8.
[29] APS Group Scotland. Drinking water quality in Scotland 2013: public water supply. Drinking Water Quality Regulator for Scotland; 2014.
[30] World Health Organization. Nutrients in drinking water. Geneva: WHO Press; 2005.
[31] Vargaftik NB, Volkov BN, Voljak LD. International tables of the surface tension of water. J Phys Chem Reference Data 1993;12(3):817–20.
[32] Xu S, Cui J, Ren X. Applied mechanics and engineering model on raindrops falling. In: International Conference on electronic and mechanical engineering and information technology, Heilongjiang; 2012.
[33] MacDonald AM, Dochartaigh B. Baseline Scotland: an overview of available groundwater chemistry data for Scotland. British Geological Survey; 2005.